Research article

Native interface of the SAM domain polymer of TEL

Hoang H Tran, Chongwoo A Kim, Salem Faham, Marie-Claire Siddall and James U Bowie*

Address: Department of Chemistry and Biochemistry UCLA Laboratory of Structural Biology and Molecular Medicine, Molecular Biology Institute, 655 Boyer Hall 611 Charles E. Young Drive, E. Los Angeles, CA 90095-1570, USA

E-mail: Hoang H Tran - htran@mbi.ucla.edu; Chongwoo A Kim - chong@mbi.ucla.edu; Salem Faham - salem@mbi.ucla.edu; Marie-Claire Siddall - msiddall@uci.edu; James U Bowie* - bowie@mbi.ucla.edu

*Corresponding author

Abstract

Background: TEL is a transcriptional repressor containing a SAM domain that forms a helical polymer. In a number of hematologic malignancies, chromosomal translocations lead to aberrant fusions of TEL-SAM to a variety of other proteins, including many tyrosine kinases. TEL-SAM polymerization results in constitutive activation of the tyrosine kinase domains to which it becomes fused, leading to cell transformation. Thus, inhibitors of TEL-SAM self-association could abrogate transformation in these cells. In previous work, we determined the structure of a mutant TEL-SAM polymer bearing a Val to Glu substitution in center of the subunit interface. It remained unclear how much the mutation affected the architecture of the polymer, however.

Results: Here we determine the structure of the native polymer interface. To accomplish this goal, we introduced mutations that block polymer extension, producing a heterodimer with a wild-type interface. We find that the structure of the wild-type polymer interface is quite similar to the mutant structure determined previously. With the structure of the native interface, it is possible to evaluate the potential for developing therapeutic inhibitors of the interaction. We find that the interacting surfaces of the protein are relatively flat, containing no obvious pockets for the design of small molecule inhibitors.

Conclusion: Our results confirm the architecture of the TEL-SAM polymer proposed previously based on a mutant structure. The fact that the interface contains no obvious potential binding pockets suggests that it may be difficult to find small molecule inhibitors to treat malignancies in this way.

Background

The proto-oncogene TEL (Translocation, Ets, Leukemia) is a transcriptional repressor that contains a C-terminal Ets family DNA binding domain; a central domain that together with co-repressors recruit histone deacetylases [1–3]; and an N-terminal SAM (sterile, alpha, motif) domain [4–6], which we have recently shown forms a polymer [7]. Chromosomal translocations in a variety of leukemias result in fusion of the SAM domain of TEL to tyrosine kinase domains such as ABL, PDGFβ and JAK2 [8–14] or to the transcriptional activators AML1 and ARNT [15–17]. In the tyrosine kinase fusions, SAM domain polymerization

leads to constitutive activation of the tyrosine kinase domains, which leads in turn to cell transformation [10,12,18,19]. Thus, compounds that block TEL-SAM polymerization could be effective in treating these leukemias. To assess the feasibility of this approach it would be useful to have a structure of the polymer.

The wild-type TEL-SAM polymer forms large insoluble aggregates, which precludes structure determination. We were, however, able to obtain a structure of a mutant TEL-SAM polymer, V80E [7]. The V80E mutation is in the center of the polymer interface and reduces the affinity of subunit association enough that the protein is relatively soluble above pH 7.0, where the Glu side chain is deprotonated. Sufficient affinity remains, however, that upon crystallization, the polymer reforms in the crystal. The structure of the V80E mutant TEL-SAM revealed a helical head-to-tail polymer in which the interface is made from two different surfaces on the protein. One binding surface, the mid-loop (ML) surface, consists of residues near the middle of the protein and the second surface, the end-helix (EH) surface, is centered around the C-terminal helix. Although the V80E mutant self-associates weakly under the high pH conditions used for crystallization, we were able to show that the native interface is quite strong. In particular, a protein with a mutation in the EH surface (V80E) could bind with high affinity (K_d = 2 nM) to a protein with a mutation in the ML surface (A61D) to form a heterodimer with a native interface. In addition, the wild-type protein forms fibers, visible by electron microscopy, that have a similar width to the V80E mutant polymer we observed in the crystal.

While the wild-type and V80E mutant SAM domains form fibers that are grossly similar, we cannot be certain that the mutation does not significantly alter the interface. Even a small change in subunit orientation could result in substantial alteration of the structure of the polymer, when propagated over many subunits. We have therefore determined the structure of a heterodimer with a native interface.

Results and Discussion
Crystal structure of the TEL-SAM dimer
We first attempted to grow crystals of the V80E/A61D heterodimer characterized previously [7], but only obtained crystals of low quality. We therefore attempted to crystallize other variants and were able to obtain high quality crystals of a V80R/A61D heterodimer. The protein complex crystallized in space group P1 with cell dimensions a= 52.8 b= 60.3 c= 62.3 α = 116.2 β = 98.9 γ= 98.7. There were three dimers in the asymmetric unit. The structure was solved by molecular replacement using AMORE [20] and refined to an R_{free} = 27.2 at 2.3 Å resolution. Details

Table 1: Crystallographic data.

Space Group	P1
Resolution Limits (Å)	2.30–500.0
Cell	a = 52.8; b = 60.3; c = 62.3; α = 116.2; β = 98.9; γ = 98.7
Completeness (%)	97.5 (95.6)
Rmerge (%)	8.7 (33.5)
I/σ	12.3 (2.1)
R-factor	23.0
R_{free}	27.2
R.M.S. differences	
Bond Length	0.0061
Bond Angle	1.14
Non- protein molecules	
Water	115
Sulfates	11

Numbers in parentheses refer to the highest resolution shell (2.38 to 2.30 Å) $R_{merge} = \Sigma \mid I - <I> \mid / \Sigma <I>$, where I is the observed intensity and $<I>$ is the average intensity from observations of symmetry-related reflections. $R_{factor} = \Sigma \mid F_{obs} - F_{calc} \mid / \Sigma F_{obs}$, where F_{obs} and F_{calc} are the observed and calculated structure factor amplitudes, respectively. R_{free} is calculated for a set of reflections (10%) that were not included in atomic refinement.

of the structure determination and refinement are given in Table 1I.

The structures of the three heterodimers in the crystal are essentially identical, with an average RMSD of 0.68 Å on all atoms. A representative heterodimer is shown in Fig. 1A. As shown in Fig. 1B, the interface of the dimers consists of an apolar core comprised of Met57, Ala61, Leu64, and Leu65 on the ML surface and Phe45, Leu47, Val80 and Leu84 on the EH surface. The same residue positions make up the core of the V80E mutant structure [7].

As in the V80E structure, a network of salt-bridges surrounds the apolar core. The specific interactions in the salt-bridge network are somewhat variable and differ slightly from the V80E structure. In the structure of the native interface dimer reported here, all three dimers in the asymmetric unit contain salt-bridges from Glu44 to Lys60, Arg73 to Asp79, Asp69 to Arg71, Glu68 to Lys67, and Asp69 to Lys67. Salt-bridges from Glu56 to Arg48 and Glu68 to Arg71 were found in two of the three native interface dimers. All these salt-bridges were also observed in at least two out of the three molecules in the asymmetric unit of the V80E structure, with the exception of Glu68 to Lys67, which was surprisingly completely absent in the V80E structure [7]. Thus, while the interfaces are grossly similar in all the structures, the salt-bridging interactions are malleable, shifting to accommodate slight changes in the geometry of the subunits.
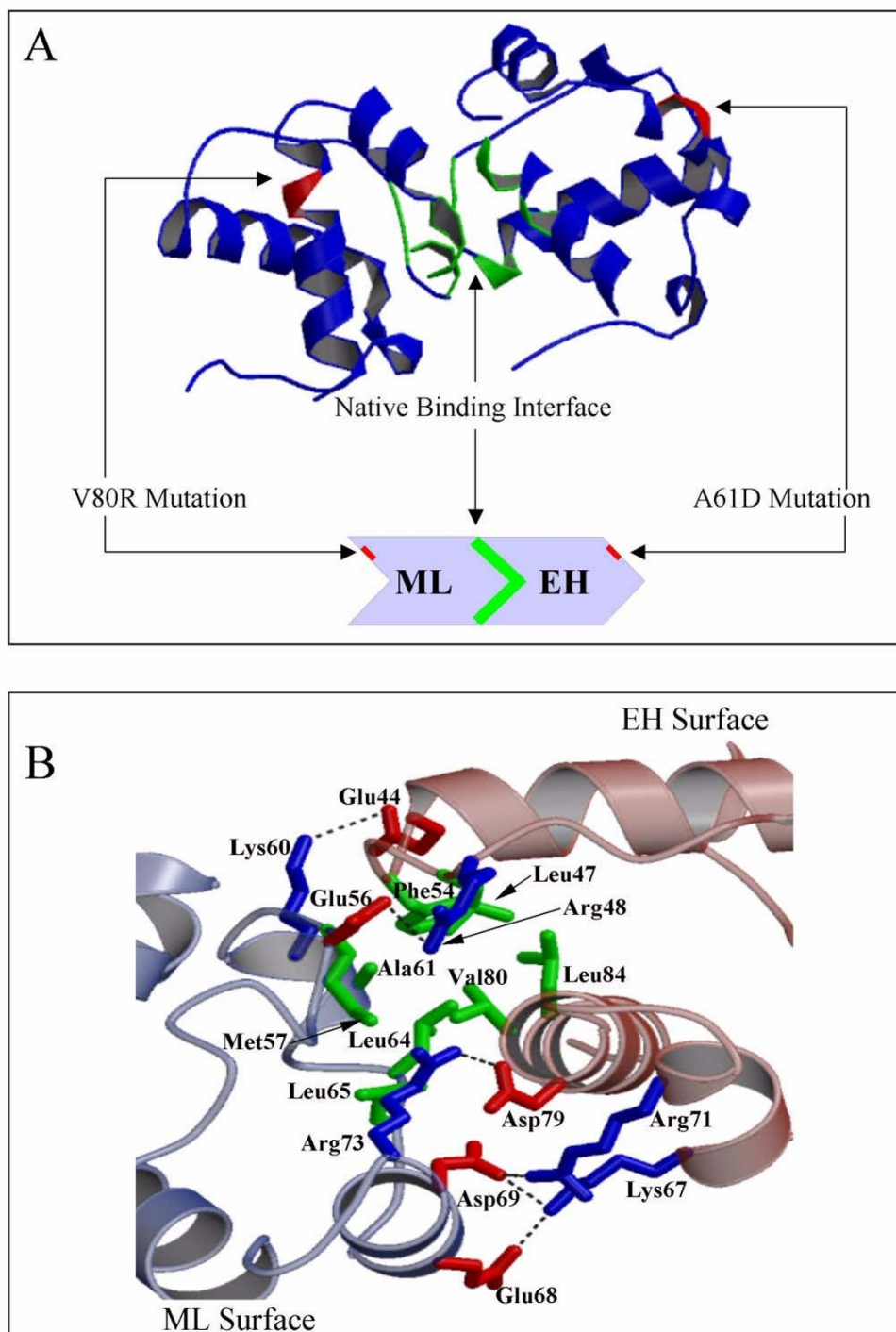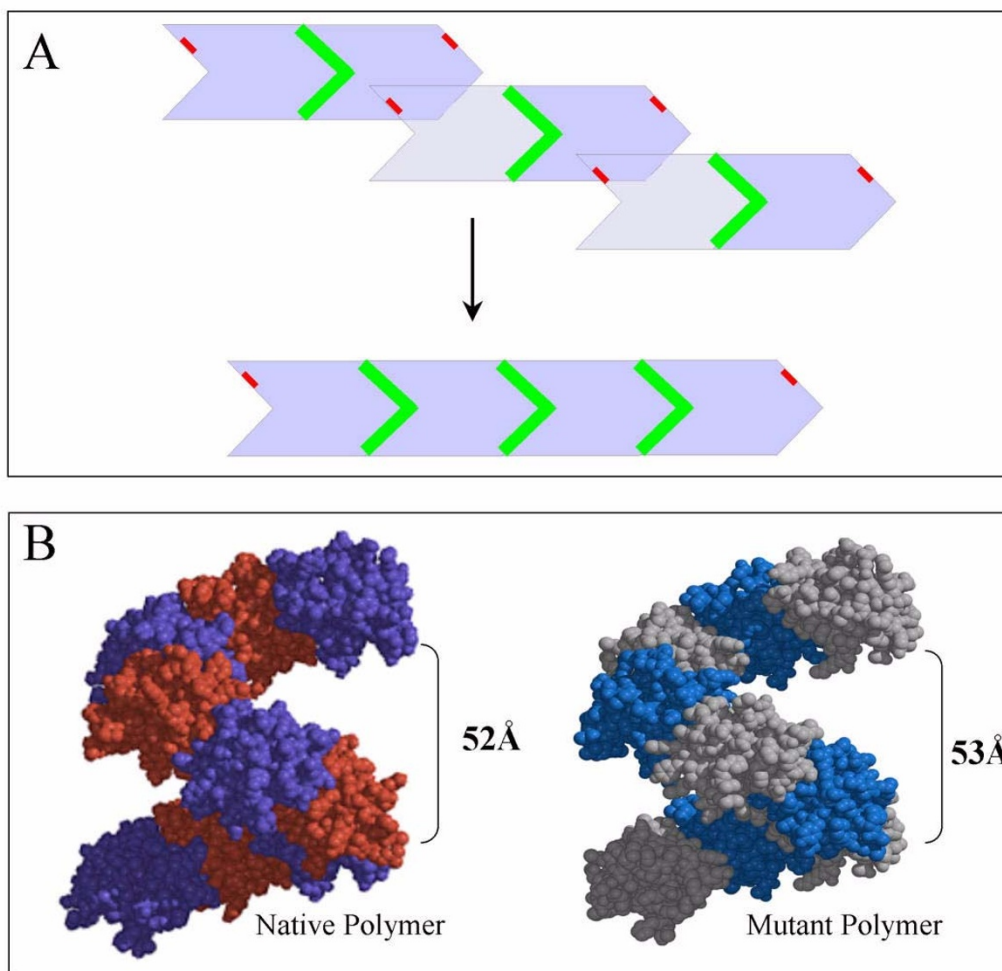
Figure 1
Structure of the heterodimer with a native interface. A) Structure of the heterodimer. Residues in the binding interface are shown in green. As shown schematically below the structure, each subunit bears a mutation in the surfaces needed to extend the polymer beyond a dimeric unit. The sites of the mutations are highlighted in red. B) A close up view of the native interface. Hydrophobic residues are colored green, negatively charged residues are in red and positively charged residues are in blue.

Figure 2
A native polymer model (A) Construction of the native polymer model. As described in the text, subunits were added by aligning the last prior subunit with the first subunit of a subsequent dimer. The second subunit of the dimer was then added to the polymer chain. (C) Native and V80E mutant polymer models. Nine subunits are shown.

Construction of native polymer model

Although it is not possible to obtain a high-resolution structure of the wild-type polymer experimentally, we can construct a model of the wild-type polymer by stringing together repeated copies of the heterodimer structure. This assumes that the structural relationship between subunits is not very flexible. The rigidity of the interface is borne out by the fact that the structure of three dimers in the asymmetric unit and the structure of the mutant V80E (see below) are so similar. The procedure for constructing a wild-type polymer model is shown schematically in figure 2A. Starting with a single subunit, additional subunits were added by aligning a subunit of the heterodimer to

the last subunit of the existing polymer chain. The new subunit was then added to the existing chain. This procedure was used to construct three different polymers using the three dimers in the crystal asymmetric unit. The resulting polymers were essentially identical with an RMSD on polymers of nine subunits of 0.87 Å on backbone atoms. The architecture of one of the resulting polymer structures is shown in Fig. 2B.

The wild-type polymer is similar to its mutant counterpart

The wild-type and V80E mutant polymers are also very similar as shown in Figure 2B. Both polymers contain SAM subunits arranged as a left-handed helix with a 6_5

screw symmetry. The repeat distance of the polymers is essentially identical, differing by only one angstrom (53 Å for mutant and 52 Å for wild-type). These results confirm the architecture of the wild-type polymer proposed previously based on the V80E mutant structure.

SAM interface as possible drug target

SAM domain oligomerization is the key event that triggers a variety of leukemias [21] and is therefore an attractive target for therapeutic intervention. Compounds that inhibit SAM association could be effective in preventing activation of the aberrant SAM/tyrosine kinase fusions and consequent cell transformation. Deep pockets on a protein surface make ideal sites for the binding of small molecule inhibitors because the surface area available for binding can be maximized [22]. Figure 3 shows the interacting surfaces of the SAM domain in the polymer. There are no obvious deep pockets for design of small molecule inhibitors.

Conclusion

In this report we have extracted a TEL-SAM dimer from the wild-type polymer and present its crystal structure. The native interface was found to be similar to the previously solved mutant interface. We also constructed a model of the native polymer and found it to be similar to the previously proposed mutant polymer. Thus, the polymer architecture is sufficiently robust to withstand a mutation from a hydrophobic to a charged residue in the center of the subunit interface. We have recently determined the polymer structure of the SAM domain from another protein involved in transcriptional repression, the polycomb group protein polyhomeotic (Ph) [Kim et al., in press]. The Ph-SAM polymer is quite similar to the TEL-SAM polymer even though the proteins have an unrelated domain structure and show less than 20% sequence identity between the SAM domains. Moreover, different residues are involved in the inter-subunit interactions. We therefore speculate that the polymer architecture is conserved for an important role in transcriptional repression, possibly involving in the generation of a repressed chromatin structure [7]. A rigid, well-defined polymer structure may be important for organizing chromatin in this manner.

From the structure, we found that the interacting surfaces of the SAM domains are devoid of the deep pockets that are ideal for small molecule binding. Although it may still be possible to find small molecule inhibitors, these results are not encouraging. Perhaps a more effective strategy would be to develop protein inhibitors, such as the mutant SAM domains described here, that can bind with high affinity and block polymerization. This strategy is currently being tested.
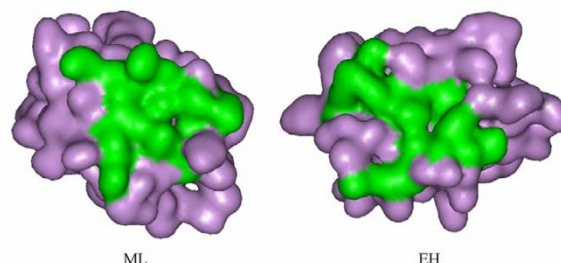

Figure 3
The interacting surfaces. The ML surface is shown on the left and the EH surface is shown on the right. Residues in the interacting surfaces are shown in green.

Materials and Methods

Protein expression, mutagenesis and purification

We used the Quickchange kit (Stratagene) to generate site directed mutants, V80R and A61D from wild-type TEL-SAM cloned into a modified pET3c vector (Novagen) [7]. The expressed protein sequence includes an MEKTR leader sequence, followed by residues 38–124 of the TEL protein and then a C-terminal His tag. Recombinant V80R and A61D mutants were expressed in E. Coli BL21 (DE3) pLysS cells (Novagen), and purified by Ni-NTA (Qiagen) and HiTrap SP (Pharmacia) affinity column chromatography followed by ammonium sulfate precipitation as described by Kim et al [7].

Crystallization, data collection and refinement

To generate the native dimer, equal amounts of each mutant dimer (both at 15 mg/ml) were mixed together prior to crystallization. Crystals were grown by the hanging drop method in which 2 µl of the 7.5 mg/ml dimer solution in 10 mM bis tris propane (pH 8.5) and 200 mM Na-Cl, were mixed with 2 µl of reservoir solution containing 5% PEG 4000 and 2.0 M ammonium sulfate. Hexagonal rod-like crystals grew at room temperature over a six-week period. Crystals were cryo-protected with the reservoir solution enriched with 30% (w/v) glycerol before data collection under a liquid nitrogen stream. The data was processed with DENZO/SCALEPACK [23]. The molecular replacement solution was found using AMORE [20] with a previously solved TEL-SAM mutant (V80E) dimer structure as the search model. The program O [24] was used for model building and CNS [25] was used for refinement. Water molecules and sulfates were added to the model near the end of refinement using difference electron den-

sity maps. The final model has a crystallographic R-factor (Rcryst) of 23.0% and R-free of 27.2% on 10% of the data (Table 1). The program O was also used for subsequent construction of the native polymer.

Coordinates

Coordinates have been deposited in the Protein Data Bank (Accession Code 1LKY).

Acknowledgements

References

1. Chakrabarti SR, Nucifora G: **The leukemia-associated gene TEL encodes a transcription repressor which associates with SMRT and mSin3A.** *Biochem Biophys Res Commun* 1999, **264:**871-7
2. Guidez F, Petrie K, Ford AM, Lu H, Bennett CA, MacGregor A, Hannemann J, Ito Y, Ghysdael J, Greaves M, Wiedemann LM, Zelent A: **Recruitment of the nuclear receptor corepressor N-CoR by the TEL moiety of the childhood leukemia-associated TEL-AML1 oncoprotein [In Process Citation].** *Blood* 2000, **96:**2557-61
3. Fenrick R, Amann JM, Lutterbach B, Wang L, Westendorf JJ, Downing JR, Hiebert SW: **Both TEL and AML-1 contribute repression domains to the t(12;21) fusion protein.** *Mol Cell Biol* 1999, **19:**6566-74
4. Kyba M, Brock HW: **The SAM domain of polyhomeotic, RAE28, and scm mediates specific interactions through conserved residues.** *Dev Genet* 1998, **22:**74-84
5. Ponting CP: **SAM: a novel motif in yeast sterile and Drosophila polyhemeotic proteins.** *Protein Sci* 1995, **4:**1928-30
6. Schultz J, Ponting CP, Hofmann K, Bork P: **SAM as a protein interaction domain involved in developmental regulation.** *Protein Sci* 1997, **6:**249-53
7. Kim CA, Phillips ML, Kim W, Gingery M, Tran HH, Robinson MA, Faham S, Bowie JU: **Polymerization of the SAM domain of TEL in leukemogenesis and transcriptional repression.** *EMBO J* 2001, **20:**4173-4182
8. Eguchi M, Eguchi-Ishimae M, Tojo A, Morishita K, Suzuki K, Sato Y, Kudoh S, Tanaka K, Setoyama M, Nagamura F, Asano S, Kamada N: **Fusion of ETV6 to neurotrophin-3 receptor TRKC in acute myeloid leukemia with t(12;15)(p13;q25).** *Blood* 1999, **93:**1355-63
9. Golub TR, Barker GF, Lovett M, Gilliland DG: **Fusion of PDGF receptor beta to a novel ets-like gene, tel, in chronic myelomonocytic leukemia with t(5;12) chromosomal translocation.** *Cell* 1994, **77:**307-16
10. Golub TR, Goga A, Barker GF, Afar DE, McLaughlin J, Bohlander SK, Rowley JD, Witte ON, Gilliland DG: **Oligomerization of the ABL tyrosine kinase by the Ets protein TEL in human leukemia.** *Mol Cell Biol* 1996, **16:**4107-16
11. Knezevich SR, McFadden DE, Tao W, Lim JF, Sorensen PH: **A novel ETV6-NTRK3 gene fusion in congenital fibrosarcoma.** *Nat Genet* 1998, **18:**184-7
12. Lacronique V, Boureux A, Valle VD, Poirel H, Quang CT, Mauchauffe M, Berthou C, Lessard M, Berger R, Ghysdael J, Bernard OA: **A TEL-JAK2 fusion protein with constitutive kinase activity in human leukemia.** *Science* 1997, **278:**1309-12
13. Papadopoulos P, Ridge SA, Boucher CA, Stocking C, Wiedemann LM: **The novel activation of ABL by fusion to an ets-related gene, TEL.** *Cancer Res* 1995, **55:**34-8
14. Peeters P, Raynaud SD, Cools J, Wlodarska I, Grosgeorge J, Philip P, Monpoux F, Van Rompaey L, Baens M, Van den Berghe H, Marynen P: **Fusion of TEL, the ETS-variant gene 6 (ETV6), to the receptor-associated kinase JAK2 as a result of t(9;12) in a lymphoid and t(9;15;12) in a myeloid leukemia.** *Blood* 1997, **90:**2535-40
15. Golub TR, Barker GF, Bohlander SK, Hiebert SW, Ward DC, Bray-Ward P, Morgan E, Raimondi SC, Rowley JD, Gilliland DG: **Fusion of the TEL gene on 12p13 to the AML1 gene on 21q22 in acute lymphoblastic leukemia.** *Proc Natl Acad Sci USA* 1995, **92:**4917-21
16. Romana SP, Mauchauffe M, Le Coniat M, Chumakov I, Le Paslier D, Berger R, Bernard OA: **The t(12;21) of acute lymphoblastic leukemia results in a tel-AML1 gene fusion.** *Blood* 1995, **85:**3662-70
17. Salomon-Nguyen F, Della-Valle V, Mauchauffe M, Busson-Le Coniat M, Ghysdael J, Berger R, Bernard OA: **The t(1;12)(q21;p13) translocation of human acute myeloblastic leukemia results in a TEL-ARNT fusion.** *Proc Natl Acad Sci USA* 2000, **97:**6757-62
18. Carroll M, Tomasson MH, Barker GF, Golub TR, Gilliland DG: **The TEL/platelet-derived growth factor beta receptor (PDGF beta R) fusion in chronic myelomonocytic leukemia is a transforming protein that self-associates and activates PDGF beta R kinase-dependent signaling pathways.** *Proc Natl Acad Sci USA* 1996, **93:**14845-50
19. Jousset C, Carron C, Boureux A, Quang CT, Oury C, Dusanter-Fourt I, Charon M, Levin J, Bernard O, Ghysdael J: **A domain of TEL conserved in a subset of ETS proteins defines a specific oligomerization interface essential to the mitogenic properties of the TEL-PDGFR beta oncoprotein.** *EMBO J* 1997, **16:**69-82
20. Navaza J: **Implementation of molecular replacement in AMoRe.** *Acta Crystallographica Section D Biological Crystallography* 2001, **57:**1367-1372
21. Rubnitz JE, Pui CH, Downing JR: **The role of TEL fusion genes in pediatric leukemias.** *Leukemia* 1999, **13:**6-13
22. Kuntz ID: **Structure-based strategies for drug design and discovery.** *Science (Washington D C)* 1992, **257:**1078-1082
23. Otwinowski Z, Minor W: *Methods Enzymol* 1997, **276:**307-326
24. Perrakis A, Morris R, Lamzin VS: **Automated protein model building combined with iterative structure refinement.** *Nat Struct Biol* 1999, **6:**458-463
25. Brunger AT, Adams PD, Clore GM, DeLano WL, Gros P, Grosse-Kunstleve RW, Jiang JS, Kuszewski J, Nilges M, Pannu NS, Read RJ, Rice LM, Simonson T, Warren GL: **Crystallography & NMR system: A new software suite for macromolecular structure determination.** *Acta Crystallogr D Biol Crystallogr* 1998, **54:**905-21